

## Research Article

# Structural Phenomenon of Cement-Based Composite Elements in Ultimate Limit State

I. Iskhakov and Y. Ribakov

Department of Civil Engineering, Ariel University, 40700 Ariel, Israel

Correspondence should be addressed to Y. Ribakov; ribakov@ariel.ac.il

Received 7 March 2016; Revised 27 July 2016; Accepted 28 July 2016

Academic Editor: Ana S. Guimarães

Copyright © 2016 I. Iskhakov and Y. Ribakov. This is an open access article distributed under the Creative Commons Attribution License, which permits unrestricted use, distribution, and reproduction in any medium, provided the original work is properly cited.

Cement-based composite materials have minimum of two components, one of which has higher strength compared to the other. Such materials include concrete, reinforced concrete (RC), and ferrocement, applied in single- or two-layer RC elements. This paper discusses experimental and theoretical results, obtained by the authors in the recent three decades. The authors have payed attention to a structural phenomenon that many design features (parameters, properties, etc.) at ultimate limit state (ULS) of a structure are twice higher (or lower) than at initial loading state. This phenomenon is evident at material properties, structures (or their elements), and static and/or dynamic structural response. The phenomenon is based on two ideas that were developed by first author: quasi-isotropic state of a structure at ULS and minimax principle. This phenomenon is supported by experimental and theoretical results, obtained for various structures, like beams, frames, spatial structures, and structural joints under static or/and dynamic loadings. This study provides valuable indicators for experiments' planning and estimation of structural state. The phenomenon provides additional equation(s) for calculating parameters that are usually obtained experimentally and can lead to developing design concepts and RC theory, in which the number of empirical design coefficients will be minimal.

## 1. Introduction

Behavior of structures in certain cases is similar to basic principles in human society. One of the main principles in human society is that all people are equal to each other. In other words, if, for example, there are two persons,  $N_1$  and  $N_2$ , then each of them is equal to the other and therefore  $N_1$  is not greater and not less than  $N_2$ , or

$$N_1 = N_2 = N \quad (1)$$

$$\text{or } N_1 + N_2 = 2N.$$

Let us assume that two persons,  $N_1$  and  $N_2$ , should carry  $W = 50$  kg. Then following (1), each of these persons takes 25 kg; that is,

$$W_2 = W_1 = 25 \text{ kg}, \quad (2)$$

$$W_1 + W_2 = W = 50 \text{ kg}.$$

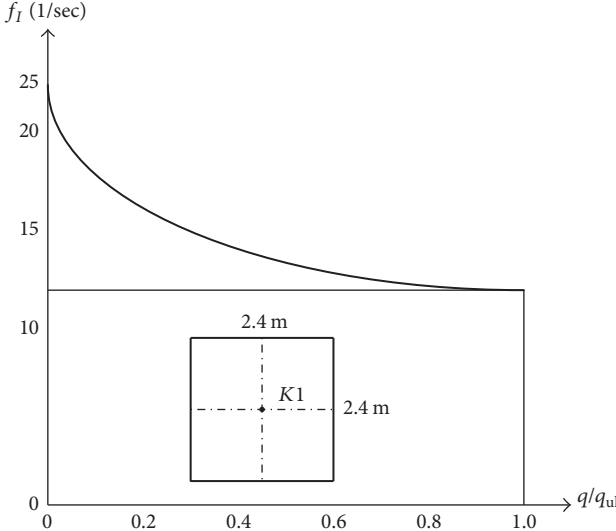
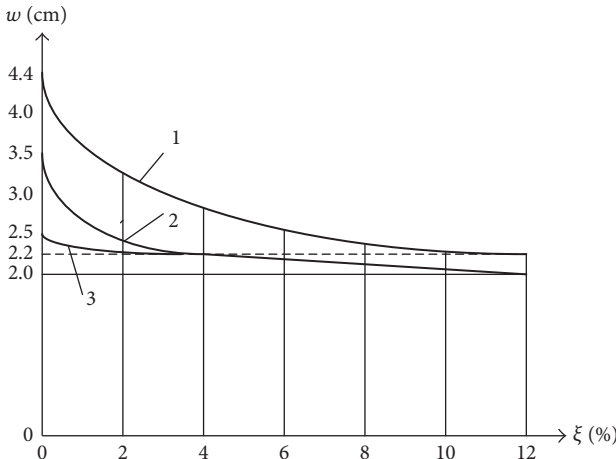
In other words,

$$W = 2W_1 = 2W_2. \quad (3)$$

It will be demonstrated in this paper that a similar principle is an objective property of a structure, made of elastic-plastic or ideally elastic-plastic material in ultimate limit state (ULS), from the load bearing capacity viewpoint. This property is further called a "structural phenomenon." The essence of this phenomenon is that values of some parameters of the structure that are measured experimentally under static or/and dynamic loadings increase or decrease by about a factor of two. Therefore, an alternative name of this phenomenon is doubling of structural design parameter at ULS.

A scheme of the principle for a general case is presented in Figure 1. For example, the figure presents dependence of dominant vibration mode frequency of a 1 : 10 scaled model of a  $24 \times 24$  m reinforced concrete (RC) shell versus load ratio,  $q/q_{ul}$ . Here  $q$  is the live load (the value of  $q$  is varied from 0 to  $q_{ul}$ ) and  $q_{ul}$  is its ultimate value. As it follows from the figure, at the ULS ( $q = q_{ul}$ ) the above-mentioned parameter decreases twice, relative to its initial value.

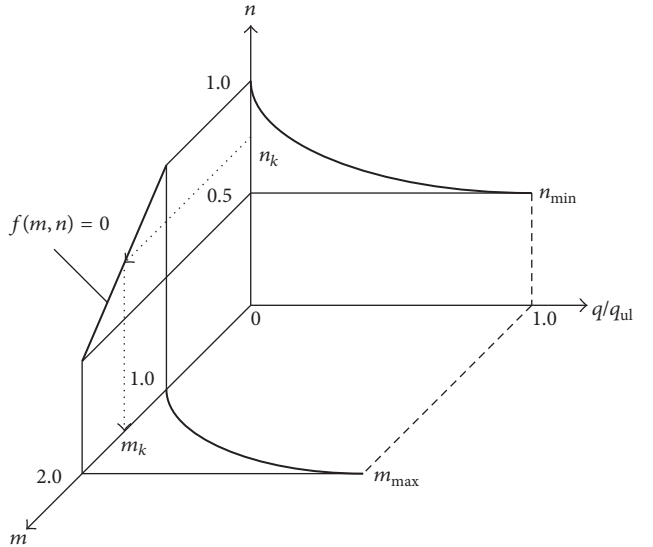
Another example that demonstrates increase in structural parameter is shown in Figure 2. A problem of increasing

FIGURE 1: Dominant technical frequency,  $f_I$ , versus load ratio,  $q/q_{ul}$ .FIGURE 2:  $24 \times 24$  m shell deflection versus damping ratio for various ground motions: 1: high-frequency earthquake, 2: medium-frequency earthquake, and 3: low-frequency earthquake.

residual deflections in a  $24 \times 24$  m RC shell under static load and additional vertical seismic excitation is considered. The following earthquakes were selected: Gazly (Uzbekistan), 1976; San Fernando (USA), 1971; and Bucharest (Romania), 1977. These earthquake records represent high-, medium-, and low-frequency ground motions, respectively. The dependence of residual deflections on damping ratio was studied (Table 1). The damping ratio,  $\xi$ , varied from 0 to 12%. The static displacement value (hidden line in Figure 2) was 2.2 cm. For a high-frequency Gazly earthquake (curve 1 in Figure 2) the residual deflections are accumulated very intensively and for  $\xi = 0$  reached 4.4 cm, which is two times higher, compared to the static value. A similar result was obtained for a medium frequency earthquake (see Table 1 and the corresponding curve 2 in the Figure), for which the residual deflection equals 3.6 cm. However, for a low-frequency earthquake (curve 3 in the Figure) the increase in residual deflections is lower. It is because the dominant

TABLE 1: Deflections in a full scale RC shell versus damping ratios.

Earthquake type	Damping ratio, %						
	0	2	4	6	8	10	12
Low frequency	2.50	2.25	2.21	2.15	2.09	2.05	2.00
Medium frequency	3.63	2.38	2.23	2.17	2.10	2.06	2.00
High frequency	4.40	3.32	2.81	2.63	2.41	2.30	2.19

FIGURE 3: Relation between structural phenomenon and minimax principle:  $m$ : generalized “increasing” parameter,  $n$ : generalized “decreasing” parameter,  $f(m, n)$ : function, relating the parameters (conditionally shown by a straight line), and  $m_k, n_k$ : arbitrary values of the parameters.

frequency of the shell is high and comparable with that of a high-frequency earthquake.

Comparing Figures 1 and 2 leads to conclusion that decreasing twice (Figure 1) and doubling (Figure 2) in structural parameters correspond to the ULS of the structure. These limit values for the same structure can be interrelated by the minimax principle [1]. Graphical interpretation of this relation is shown in Figure 3. The curve in plane  $n$ - $o$ - $q/q_{ul}$  corresponds to the dependence from Figure 1 and the curve in plane  $m$ - $o$ - $q/q_{ul}$  to Figure 2. The minimax principle combines those curves and presents their structural interrelation, as shown in the  $n$ - $o$ - $m$  plane (it is assumed that this relation is linear). Thus, if according to experimental data some factor is doubled it is logical to expect that another structural parameter correspondingly decreases twice.

Figure 4 shows the structural phenomenon evidence for a fixed concrete beam. In elastic stage,

$$|M_{el}^-| = \frac{q_{el}L^2}{12} = 2M_{el}^+, \quad (4)$$

where  $q_{el}$  is a uniformly distributed load in elastic stage ( $q_{el} \leq q_{el,ul}$ ) and  $q_{el,ul}$  is the ultimate value of this load;  $M_{el}^-$  and  $M_{el}^+$  are the maximum values of negative and positive bending moments, respectively, in beam elastic stage.

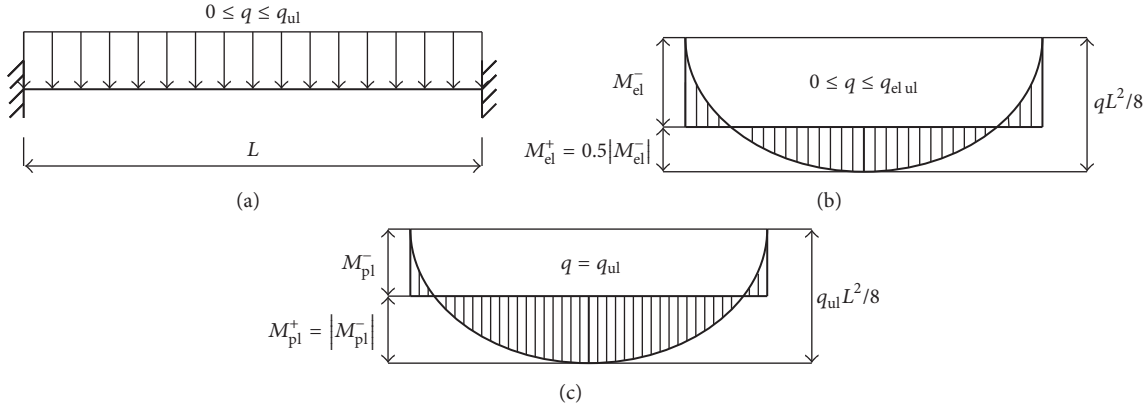


FIGURE 4: Structural phenomenon evidence for a fixed concrete beam: (a) static scheme, (b) bending moments diagram in elastic stage, and (c) bending moments diagram in ultimate limit state.

In the ULS after the moments' redistribution,

$$|M_{pl}^-| = \frac{q_{ul}L^2}{16} = M_{pl}^+, \quad (5)$$

where  $q_{ul}$  is a uniformly distributed load in ULS and  $M_{pl}^-$  and  $M_{pl}^+$  are the maximum values of negative and positive bending moments, respectively.

In both cases,

$$|M^-| + M^+ = \frac{qL^2}{8}. \quad (6)$$

Thus,

$$2 \geq \frac{|M^-|}{M^+} \geq 1. \quad (7)$$

The examples that were presented in this chapter are not the only ones. Other relevant cases will be discussed below. It should be mentioned that, as the structural phenomenon was not investigated previously, there is a very limited number of publications, in which relevant experimental data were obtained, but not analyzed. For example, experimental results [2] show that using steel fibers in concrete increases transverse deformations about two times (from  $(0.16, \dots, 0.20)\varepsilon_c$  to  $0.40\varepsilon_c$ , where  $\varepsilon_c$  is the longitudinal deformation of the structure), but it is not emphasized by the researchers.

Four-point static tests in ultimate stages show that steel fibers increase the deflections in the middle-span of a high strength concrete bending element approximately twice [3]: the deflections in beams made of concrete class C140 were 44 and 84 mm without and with steel fibers, respectively. For beams made of concrete class C200 adding steel fibers has increased the deflections from 33 to 59 mm. As in the previous example, the fact of doubling the middle-span deflections was not emphasized.

## 2. Minimax Principle in Ultimate Limit State of Structures

*2.1. Short Review of Ultimate Limit State and Minimax Principle.* The ultimate equilibrium method, proposed by

Gvozdev in 1938 [5], was a logical development of basic experimental and theoretical investigations, carried out by outstanding researchers as Galilei, Coulomb, Bach, Graf, and others [6]. This method is still used for calculating structures at ultimate limit state (load bearing capacity).

Following modern design codes, methods, based on plastic analysis, are suitable for checking structures at ultimate limit state [7]. The method is constantly developed. For a specific structure there is an exact correspondence between the external loads' system and internal forces' distribution. Just in this case the structure may transform into a mechanism [8].

Later the ultimate equilibrium method was enlarged for application in structures that are made of concrete type materials with downloading branch in the stress-strain diagram [9].

Following Gvozdev [5], there are three theorems of the ultimate equilibrium method:

- (i) static theorem, estimating the lower bound of the ultimate loading capacity of the structure,
- (ii) kinematic theorem, estimating the upper bound of the ultimate loading capacity of the structure,
- (iii) unity theorem that could directly obtain the ultimate loading capacity but does not allow finding the maximum static or minimum kinematic loads.

It should be mentioned that the required ductility of an RC structure or its element should be sufficient for the suggested failure mechanism.

Series of experiments were performed in the previous century in order to overcome the problem of the unity theorem and to find a more accurate value of the structural load bearing capacity [10]. The experimental investigations were focused on studying the structures made of physically nonlinear materials (ferrocement and reinforced concrete). The obtained experimental data allows calculation of the load bearing capacity by static or kinematic theorems and realizes the unity theorem.

Another possible way for exact estimation of RC structures' load bearing capacity is simultaneous application of

the static and kinematic methods at the ULS. However, this way is not practical, because it is impossible to estimate the convergence of results, obtained by these methods [1]. It is suitable just for rather simple structural schemes (even for continuous beams it is not always applicable). Additionally, if condition (1) is not satisfied, the fields of internal plastic forces,  $F$ , and possible displacements,  $w$ , should be changed, but convergence of this process is still not proved.

Development of this idea yielded to minimax principle formulation [1]. The essence of this principle is realization of genuine bearing capacity of the structure (avoiding the lower and/or upper bounds estimation). With this aim it is proposed to use both extreme properties of the structures failure load (static and kinematic) simultaneously in the calculation process. In this case just one calculation (static or kinematic) is carried out. Thus, the minimax principle became indeed an apparatus for realization of the unity theorem. This apparatus logically unifies the extreme (static and kinematic) theorems of the ultimate limit equilibrium method.

The authors have shown that the minimax term means minimum of maxima or the lowest board of upper bounds for a two-variable function of the structural bearing capacity [1]. It should be mentioned that at the same time the maximum or the upper bound are found according to one of the variables (e.g., kinematic parameter) for a fixed value of the second variable (e.g., static parameter). After that the value of the second parameter is changed and the above described process is repeated.

**2.2. Quasi-Isotropy as a Limit State of RC Element.** Let us consider a rectangular RC element section that contains reinforcing  $A_s$  in tensile zone and  $A'_s$  in the compression one.  $A_s$ ,  $A'_s$ , and the concrete compressed zone height,  $x$ , are unknown. Two static equilibrium equations are not enough to determine the above specified unknowns. Hence, an additional condition should be found.

A quasi-isotropic state requires minimal total reinforcing of the section: that is,  $(A_s + A'_s) \rightarrow \min$ . It can be shown that in this case the relative section compression zone depth,  $\omega$ , reaches its extremal value  $0.5(1 + d'_s/d)$ , where  $d'_s$  and  $d$  are the protective concrete layer for  $A'_s$  and the section effective depth, respectively. In a common case of a section with a vertical symmetry axis  $\omega_{\text{extr}} = 1 - S_0/(dA_0) + d'_s/(2d)$ , where  $S_0$  is the first moment of an effective section and  $A_0$  is the effective section's area.

Let us calculate, for example, an RC element with rectangular section of  $b \times h = 250 \times 500$  mm,  $d_s = d'_s = 40$  mm, steel design strength  $f_{sd} = 350$  MPa, concrete design strength  $f_{cd} = 10$  MPa, and the external forces moment  $M_d = 250$  kNm. For the reinforcement sections in the tensile and compressed zones and the total reinforcement section as a function of the compressed zone's relative depth,  $\omega_{\text{extr}} = 0.5(1 + d'_s/d) = 0.5(1 + 40/460) = 0.543$ .

Graphical representation of the three above functions is given in Figure 5, where  $2d'_s/d \leq \omega \leq \omega_{\text{extr}}$ . Increasing  $\omega$  yields increase of  $A_s$  and decrease of  $A'_s$ . The total

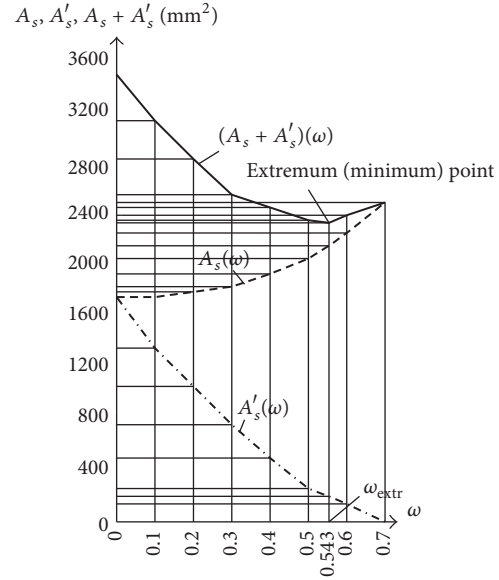


FIGURE 5: Minimization of total RC section reinforcement ( $A_s + A'_s$ ).

reinforcement ( $A_s + A'_s$ ) decreases until  $\omega$  reaches  $\omega_{\text{extr}}$  value, and then it increases. In the same time,  $\omega > \omega_{\text{extr}}$  should be avoided; otherwise, according to the concrete theory, the section's collapse will be brittle. When  $(A_s + A'_s)$  is minimum, and  $\omega = \omega_{\text{extr}}$ , the section is quasi-isotropic. In other words, a quasi-isotropic section stage yields optimal (minimum) total reinforcement section.

### 3. Analysis of the Structural Phenomenon Based on Original Experimental and Theoretical Data

The present study is based on selected experimental and theoretical data that were reported by many researchers in the last three decades of the previous century and till today. As known, very many researchers have investigated behavior of structures under loads that increase from elastic state up to its failure. In this case if a structure is symmetric and the load is also symmetric, usually structural parameters in elastic state increase or decrease twice at failure. Therefore, we have presented and analyzed indeed those data.

It is logical to analyze the structural phenomenon from the following three different groups of experiments:

- (i) investigation of structural concrete at material level,
- (ii) behavior of RC structures and elements under static loads,
- (iii) response of RC structures and elements to dynamic loads.

**3.1. Structural Concrete as Material.** Using high strength concrete in construction became very popular in recent decades. At the same time, the following fact is evident: in spite of the fact that concrete compressive strength increases

with concrete class, the mean value of concrete tensile deformations,  $\varepsilon_{ctm}$ , reaches its maximum for concrete class C 70 and remains constant for higher concrete classes [7]. Moreover, the maximum value of  $\varepsilon_{ctm}$  is about  $1.2 \cdot 10^{-4}$ , and for the lowest structural concrete class it is about  $0.6 \cdot 10^{-4}$ . It is one of the structural phenomenon evidences, as

$$\frac{\varepsilon_{ctm \text{ max}}}{\varepsilon_{ctm \text{ min}}} = 2. \quad (8)$$

As an extension of this idea, let us discuss the relation between the displacements and Poisson deformations under ultimate load and after unloading of two-layer beams consisting of normal and fibered high strength concrete in tensile and compression zones, respectively [11]. Following experimental results for full-scale 3 m beams, tested using four-point loading, the mid span displacement under the ultimate load was 35 mm and the residual deflection was about 18 mm. The corresponding Poisson deformations were about  $0.65 \cdot 10^{-3}$  and  $0.32 \cdot 10^{-3}$ . A similar behavior was observed for horizontal shear deformations between the concrete layers. The maximum deformations under the ultimate load were  $2.7 \cdot 10^{-3}$ , whereas the residual ones were about  $1.25 \cdot 10^{-3}$ .

Following modern codes ([7, 12], etc.), the maximum elastic deformations of normal strength concrete,  $\varepsilon_{c \text{ el ul}}$ , are about  $1 \cdot 10^{-3}$ , which corresponds to the initial modulus of elasticity for short term loading (without considering durability aspects),  $E_{c1} = \tan \alpha_1$  (slope of line  $oa$  in Figure 6). The ultimate plastic deformation  $\varepsilon_{c \text{ pl ul}}$  is  $2 \cdot 10^{-3}$ . If concrete would behave elastically up to  $\varepsilon_{c \text{ pl ul}}$  (line  $ob$  in the figure), a corresponding modulus of elasticity is  $E_{c2} = \tan \alpha_2$ . It is easy to show that

$$E_{c1} = 2E_{c2}. \quad (9)$$

It demonstrates again the same phenomenon that, when the concrete element reaches the ultimate deformation, its stiffness characteristic decreases twice.

As it was shown experimentally, increasing the load, acting on cylindrical concrete specimens with different steel fibers contents (from 0 to  $60 \text{ kg/m}^3$ ), yields increase in Poisson coefficient,  $\nu$ . It was found that the optimal fiber content is  $30 \text{ kg/m}^3$ . Following the experimental data, in specimens without fibers,  $\nu_{\min 0} = 0.11$  and  $\nu = 0.22$ . In specimens with optimal fibers content,  $\nu_{\min 30} = 0.22$  and  $\nu_{\max 30} = 0.44$ . The ratios

$$\begin{aligned} \frac{\nu_{\min 30}}{\nu_{\min 0}} &= \frac{\nu_{\max 30}}{\nu_{\max 0}} = 2, \\ \frac{\nu_{\max 30}}{\nu_{\min 30}} &= \frac{\nu_{\max 0}}{\nu_{\min 0}} = 2 \end{aligned} \quad (10)$$

demonstrate that, like in case of longitudinal deformations, also for transverse ones the parameters are doubled.

Concrete creep increases with time and correspondingly yields a decrease in the modulus of elasticity ([7, 12, 13], etc.). For example, for normal strength concrete the initial modulus of elasticity decreases twice during a five-year period [7]:

$$\frac{E_c(t=0)}{E_c(t=5 \text{ years})} = 2. \quad (11)$$

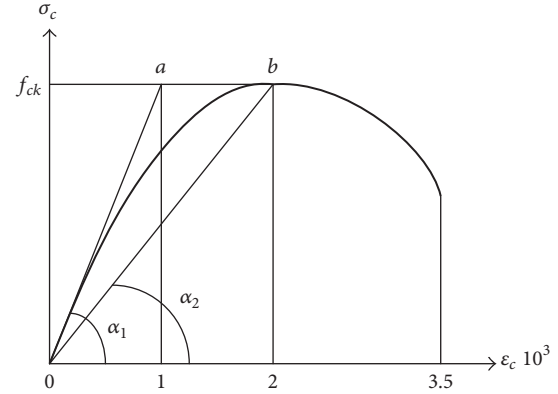


FIGURE 6: Influence of concrete element deformations on its stiffness parameter.

Additionally, concrete creep depends on the compression stress in service limit state, surrounding environment humidity, composition and class of concrete, and so forth. Considering the concrete class only, the concrete creep depends on concrete creep coefficient  $\beta_{ck}$  that decreases as the concrete class increases. Let us compare the concrete creep coefficients for the lowest and the highest structural concrete classes, C 20 and C 90, respectively, according to the equation available in Eurocode [7],

$$\beta_{cm} = \frac{16.8}{f_{cm}^2}, \quad (12)$$

where  $f_{cm}$  is a mean compressive strength of concrete. In this case, the ratio between those coefficients is

$$\frac{\beta_{cm}^{C20}}{\beta_{ck}^{C90}} = \frac{3.360}{1.697} = 1.98. \quad (13)$$

In other words, the relation between the concrete creep deformations for high strength concrete (HSC) and normal strength concrete (NSC) is

$$\varepsilon_{cr}^{NSC} \approx 2\varepsilon_{cr}^{HSC}. \quad (14)$$

Thus, using HSC allows achieving significant decrease in concrete creep deformations (up to two times).

**3.2. Behavior of RC Structures and Elements under Static Loads.** In the previous section examples of structural phenomenon for cement-based composite nonlinear material was discussed (concrete was considered as a private case of such material). The present section focused on behavior of RC elements from the viewpoint of statics. A rectangular RC bending element section with double reinforcement of  $A_s$  and  $A'_s$  in tensile and compression zones, respectively, is considered. If the element is in ULS, the reinforcement sections are

$$\begin{aligned} A'_s &= \frac{[M_d - f_{cd}bd^2\omega(1 - 0.5\omega)]}{[f_{sd}(d - d'_s)]} \\ A_s &= A'_s + \frac{f_{cd}bd\omega}{f_{sd}}, \end{aligned} \quad (15)$$

where  $M_d$  is the external forces moment;  $f_{cd}$  and  $f_{sd}$  are strength of the reinforced and reinforcing materials, respectively;  $b$  and  $h$  are the section dimensions;  $d_s$  and  $d'_s$  are concrete covering in the tensile and compression zones, respectively;  $\omega = x/d$  is the relative compression zone depth;  $x$  is the compression zone depth and  $d = h - d_s$  is the effective section height.

The reinforcement sections depend on  $\omega$  that is a third unknown in (15). To obtain  $\omega$ , the minimax principle was proposed [1, 14]:

$$(A_s + A'_s) \rightarrow \min \quad (16)$$

that corresponds to effective section reinforcement. Consequently,

$$\frac{d(A_s + A'_s)}{d\omega} = 0. \quad (17)$$

Applying condition (17) to (15), the following extremum value of  $\omega$  was obtained:

$$\omega_{\text{extr}} = 0.5 \left( 1 + \frac{d'_s}{d} \right). \quad (18)$$

Taking into account that the order of  $d'_s$  is lower than that of  $d$ , the second term in the brackets can be neglected and the extremum value of the relative compression zone depth is

$$\begin{aligned} \omega_{\text{extr}} &= 0.5; \\ h &= 2\omega_{\text{extr}}d. \end{aligned} \quad (19)$$

It means that for optimal reinforcement of the considered section the concrete compression zone depth should be equal to half of the total section height. In this case, an anisotropic RC section becomes a quasi-isotropic one [14]. In other words, the structural phenomenon corresponds to optimal design concept of cement-based composite bending elements. Similar results were obtained for eccentrically loaded elements in compression and tension with large eccentricities.

A sum of the bending moment, taken by the compressed reinforcement,  $\Delta M$ , and the maximal moment taken by the tensile reinforcement,  $M_s \max$ , is equal to the external bending moment,  $M_d$ . In order to carry the maximum value of this moment,  $M_d \ max$ , the section of  $A'_s$  can be obtained from the condition that the corresponding moment  $\Delta M_{\max}$  will not exceed that taken by the compressed concrete zone,  $M_c \ max$ . In other words, the force in compressed reinforcement is

$$A'_{s \ max} f_{sd} \leq x_{\max} b f_{cd}. \quad (20)$$

In the ULS these forces are equal and therefore

$$\begin{aligned} \Delta M_{\max} &= M_c \ max; \\ \Delta M_{\max} + M_c \ max &= 2M_c \ max. \end{aligned} \quad (21)$$

Thus, the maximum value of the compressed reinforcement section corresponds to the condition, when

$$M_d \ max = 2M_c \ max = 2M_s \ max. \quad (22)$$

At the same time (19) is valid; that is, brittle section failure is avoided. It can be concluded that an RC section that behaves as quasi-isotropic one can be strengthened by compression reinforcement up to achieving a double maximum moment bearing capacity of a section with single reinforcement.

The phenomenon, related to doubling of various structural parameters, is also evident in problems of section design to shear forces [15]. It is known that ultimate shear resistance is determined as

$$V_{Rd \ max} = V_{Rdc} + V_{Rds}, \quad (23)$$

where  $V_{Rdc}$  is the concrete shear bearing capacity and  $V_{Rds}$  is shear resistance provided by shear reinforcement.

Following modern codes [7, 16],

$$\begin{aligned} V_{Rds} &\leq V_{Rdc}; \\ \max V_{Rds} &= V_{Rdc}. \end{aligned} \quad (24)$$

Therefore, the maximum section shear bearing capacity is

$$V_{Rd \ max} = 2V_{Rdc}. \quad (25)$$

The main parameters, affecting the section shear bearing capacity, are angles  $\alpha$  and  $\theta$ , defining, respectively, the links' inclination and the main compression stresses in concrete [7, 15]. Moreover, relation between these angles is also important. The angle  $\alpha$  is arbitrary selected by designer, according to constructive and technological requirements, whereas  $\theta$  depends on  $\alpha$ .

A theoretical value of  $\theta$  can be obtained using minimax principle [1], based on simultaneous minimization of ultimate external loading and maximization of internal stresses. The ultimate shear force is maximized in the following additional equation:

$$\frac{dV_{Rd \ max}}{d\theta} = 0. \quad (26)$$

Thus, the extreme value of  $\theta$  that maximizes the section shear force is obtained as follows [1]:

$$\begin{aligned} \theta_{\text{extr}} &= 0.5\alpha; \\ \alpha &= 2\theta_{\text{extr}}. \end{aligned} \quad (27)$$

Consequently, when the section reaches its ultimate shear bearing capacity, the angle of links,  $\alpha$ , selected at the design stage, is equal to the doubled main compression forces angle,  $\theta_{\text{extr}}$ .

**3.3. Response of RC Structures and Elements to Dynamic Loads.** Structural phenomenon is also evident in dynamic behavior of buildings and proved by experimental data. For example, based on experimental results, obtained for a full-scale three-story beamless precast framed RC building part [17], an unloaded frame had a dominant natural vibration period  $T_{1 \ min} = 0.6$  s. The frame was subjected to impulse load steps of 30, 70, and 110 kN. At the last step the frame

behaved as a geometrically and physically nonlinear system and the corresponding dominant vibration period  $T_{1\ max} = 1.2 s. It follows that$

$$T_{1\ max} = 2T_{1\ min}. \quad (28)$$

Thus, doubling of the dominant vibration period indicates that the structure reaches significant nonlinear deformations, which characterizes the ultimate dynamic state of the structure.

The influence of gravitation stresses on RC section energy dissipation under cyclic forces was examined [18]. As the structural response in this case is nonsymmetric, the hysteretic loop area reduces, relative to the case without considering the gravitation loading. It was assumed in [18] that the maximum gravitation stress  $\sigma_{cg} = 0.5f_{ck}$ : that is, the concrete reached the maximum elastic stress. It was also assumed that under cyclic loading the section reached the plastic state. The dissipated energy in this case is significantly lower than that obtained without considering the gravitation loads:

$$U_{tot} \approx 2U_{g\ tot}, \quad (29)$$

where  $U_{tot}$  and  $U_{g\ tot}$  are the total section plastic energy dissipation without and with gravitation loads, respectively.

As the section plastic energy dissipation decreases proportionally to the gravitation stresses, the ductility factor correspondingly decreases twice.

A six floor flat slab RC building with braced frame was analyzed [4]. It was shown that disengagement of concrete braces leads to a system with variable stiffness. Reduction of modulus of elasticity leads to unilateral disengagement. Additionally, static loading countereffect appears due to dynamic loading. These factors substantially reduce the seismic forces (about twice), giving rise to a static scheme that represents the structure's most suitable response to a given earthquake.

Seven possible structural static schemes, running from fully braced to unbraced, were analyzed (Figure 7) [4]. The first and the last schemes are completely symmetric, but the first is fully braced and the last is fully unbraced. The fourth scheme represents a fully antisymmetric scheme. Following the obtained results, the dominant natural vibration periods, corresponding to those schemes, were  $T_1 = 0.248$  s,  $T_4 = 0.433$  s, and  $T_7 = 1.037$  s. Thus,

$$\begin{aligned} \frac{T_4}{T_1} &= \frac{0.433}{0.248} = 1.75; \\ \frac{T_7}{T_4} &= \frac{1.037}{0.433} = 2.39. \end{aligned} \quad (30)$$

It is evident that in this case also the average difference in the natural vibration periods is 2.07.

Following the results, obtained in the same research [4], the structural phenomenon is evident not just for dynamic parameters, but also for peak base shear forces, which were minimal for scheme 4 in Figure 7:  $V_{d4} = 557.8$  kN, whereas  $V_{d1} = 1002.0$  kN. The ratio between these shear forces is 1.8, which is about 2.

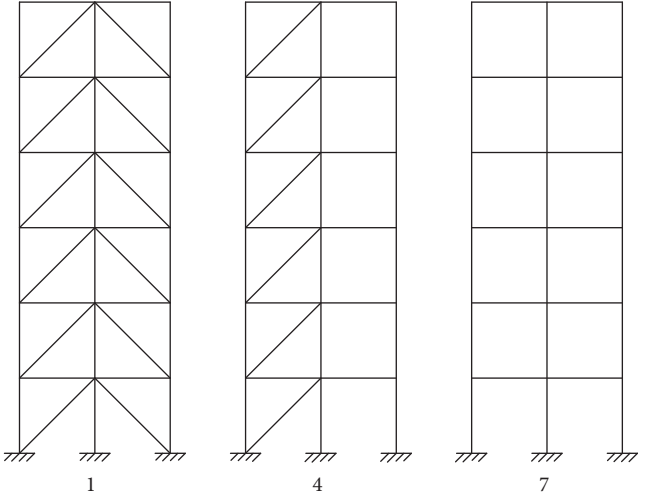


FIGURE 7: Changes in the basic frame scheme under growing horizontal dynamic loading (following [4]).

Additionally, a self-variable stiffness RC frame adapts its response to an earthquake by using the basic concrete properties [4]. The frame selects a limit state with maximum energy dissipation and the seismic forces effects decrease about twice. The system has several seismic self-control modes (in terms of material, structure, and loading), which are applied for adapting the frame to the given earthquake.

As known, it is impossible to test real full-scale structures in ULS. In most cases, structural response in limit elastic state is tested. At the same time, it is very important to know structural dynamic parameters close to the ULS. For this reason, modern numerical techniques are applied. Experimental results for the limit elastic state are effective for verification of numerically obtained initial structural parameters. The authors have shown that experimentally obtained dominant vibration period for a full-scale 9-floor RC building was 0.72 s and the corresponding base shear force (BSF) was 3400 kN [19]. The investigated structure was designed for an earthquake with peak ground acceleration  $PGA = 0.15$  g. Numerical analysis of the building subjected to the same load, like in the experiments, showed that the BSF was 3320 kN, which is very close to the value obtained based on experimental data.

For adapting the building to a region with  $PGA = 0.3$  g, a base isolation system (BIS) was used. The BIS was designed so that the BSF in the isolated building, subjected to an earthquake with  $PGA = 0.3$  g, would be close to those in a fixed-base structure under an earthquake with  $PGA = 0.15$  g [19]. Numerical results show that for the selected real earthquakes the average BSF in the isolated building is 3543 kN. The corresponding dominant natural vibration period of the isolated structure was 1.4 s; that is, it is about two times higher, relative to the fixed-base building in a limit elastic state (0.72 s). It was concluded that increasing the dominant natural vibration period of the building from 0.72 to 1.4 s (about twice) allows its adaptation to a zone with

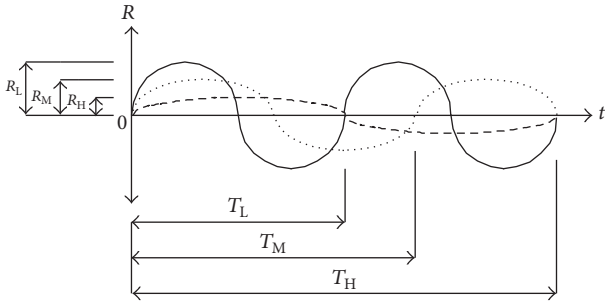


FIGURE 8: Structural dynamic response,  $R$ , versus dominant vibration period:  $T_H$ ,  $T_M$ , and  $T_L$ : dominant vibration periods for high, medium, and low structural ductility, respectively.

higher seismicity ( $\text{PGA} = 0.3 \text{ g}$  instead of  $0.15 \text{ g}$ ) and keeps its response in the same limits [19]:

$$\frac{T_{1.03 \text{ g}}}{T_{1.15 \text{ g}}} = \frac{1.4 \text{ s}}{0.72 \text{ s}} \approx 2 = \frac{0.3 \text{ g}}{0.15 \text{ g}}. \quad (31)$$

Analysis of structural ductility enables us to prove the above-mentioned conclusion. As the input seismic energy that affects the building is independent of structural dynamic parameters, especially of ductility, hence according to Figure 8, the energy (the area of the graph  $R_i$  versus  $T_i$ , where  $i = H, M$ , and  $L$ ) should be constant:

$$E_i = \int_0^{0.5T_i} R(T_i) dT_i = \text{const}; \quad i = H, M, L. \quad (32)$$

Therefore, if  $T_i$  increases,  $R(T_i)$  decreases; that is, the force that acts on the building during an earthquake becomes lower.

## 4. Conclusions

The present study is focused on analysis and discussion of available experimental and theoretical data from the viewpoint of a structural phenomenon. It was shown that the phenomenon is valid for various design parameters at ultimate limit state (ULS) of a structure or its elements. It was demonstrated that the phenomenon is evident for material properties and structure (or its elements), as well as for structural static and/or dynamic response.

The phenomenon is based on quasi-isotropic state of a structure at ULS and minimax principle. It is supported by many experimental and theoretical results, obtained for different structures (beams, frames, spatial structures, and structural joints) under static or/and dynamic loadings.

The structural phenomenon enables us

- (i) to predict the ULS of the building or appropriate safety factor to this state,
- (ii) to assess the limit changes of strength and deformation parameters in buildings before beginning their real design,
- (iii) to solve strengthening problems of a building,

- (iv) to carry out certification of a building (durability problem),
- (v) to find the limit values of steel fibers, confining effect, compressed reinforcement section in the element, and so forth,
- (vi) to find the seismic resistance of a structure, that is, the level of structural load bearing capacity under a strong earthquake,
- (vii) to reveal the stage, when the structural static scheme is changed.

The structural phenomenon, discussed and analyzed in the frame of the present study, can be also applied for other important issues in structural design. For example, one of logical suggestions for selecting an upper limit for a number of passive damping units in a structure is that maximum reduction in dynamic response of a building with effective supplemental passive devices is two times, compared to the original one (without dampers).

Thus, the results of this study provide valuable indicators for experiments planning, estimation of structural state (elastic, elastic-plastic, plastic, or failure), evaluating possibilities of retrofitting, and so forth. From the mathematical viewpoint, the phenomenon provides additional equation(s) that enable us to calculate parameters, usually obtained experimentally or using some empirical coefficients. Therefore, using this phenomenon can lead to developing proper design concepts and new RC theory, in which the number of empirical design coefficients will be minimal.

## Competing Interests

The authors declare that they have no competing interests.

## References

- [1] I. Iskhakov and Y. Ribakov, *Ultimate Equilibrium of RC Structures using Mini-Max Principle*, Nova Science, New York, NY, USA, 2014.
- [2] D. J. Dowrick, *Earthquake Resistant Design: For Engineers and Architects*, John Wiley & Sons, New York, NY, USA, 1995.
- [3] J. Magnusson and M. Hallgren, “Reinforced high strength concrete beams subjected to air blast loading,” in *Structures under Shock and Impact*, N. Jones and C. A. Brebbia, Eds., vol. 8, WIT Press, Southampton, UK, 8th edition, 2004.
- [4] I. Iskhakov and Y. Ribakov, “Seismic response of semi-active friction-damped reinforced concrete structures with self-variable stiffness,” *Structural Design of Tall and Special Buildings*, vol. 17, no. 2, pp. 351–365, 2008.
- [5] A. A. Gvozdev, “Obtaining the destructive loads value for statically indeterminate systems under plastic deformations,” in *Proceedings of the Conference on Plastic Deformations*, Russian Academy of Sciences, Moscow, Russia, 1938 (Russian).
- [6] C. Bach and O. Graf, *Tests with Simply Supported, Quadratic Reinforced Concrete Plates*, vol. 30, Deutscher Ausschuss für Eisenbeton, Berlin, Germany, 1915 (German).
- [7] Eurocode 2: Design of Concrete Structures—Part 1-1: General Rules and Rules for Buildings, 2004.

- [8] M. R. Horne, "Fundamental propositions in the plastic theory of structures," *Journal of the Institution of Civil Engineers*, vol. 34, no. 6, pp. 174–177, 1950.
- [9] A. C. Palmer, G. Maier, and D. C. Drucker, "Normality relations and convexity of yield surfaces for unstable materials or structural elements," *ASME Journal of Applied Mechanic*, vol. 34, no. 2, pp. 464–470, 1967.
- [10] I. Iskhakov, *The Limit Equilibrium of Square Shells Considering Their Deformation Scheme*, vol. 2 of *Stroitel'naya Mechanika i Rasch'yt Sooruzeniy*, Stroyizdat, Moscow, Russia, 1972 (Russian).
- [11] I. Iskhakov, Y. Ribakov, K. Holschemacher, and T. Mueller, "Experimental investigation of full-scale two-layer reinforced concrete beams," *Mechanics of Advanced Materials and Structures*, vol. 21, no. 4, pp. 273–283, 2014.
- [12] Building Code Requirements for Structural Concrete (ACI Committee 318-05), 2005.
- [13] I. Iskhakov and Y. Ribakov, "A new concept for design of fibered high strength reinforced concrete elements using ultimate limit state method," *Materials and Design*, vol. 51, pp. 612–619, 2013.
- [14] I. Iskhakov and Y. Ribakov, "Optimization of steel ratio in cement based composite bending elements," in *Proceedings of the 13th International Conference 'Mechanics of Composite Materials MSM 2004'*, Riga, Latvia, May 2004.
- [15] I. Iskhakov and Y. Ribakov, "Exact solution of shear problem for inclined cracked bending reinforced concrete elements," *Materials and Design*, vol. 57, pp. 472–478, 2014.
- [16] The Standards Institution of Israel, "SI 466 part 1, concrete code: general principles," 2012.
- [17] I. Iskhakov and Y. Ribakov, "Selecting the properties of a base isolation system based on impulse testing of a three-story structural part," *European Earthquake Engineering*, vol. 1, pp. 38–42, 2005.
- [18] I. Iskhakov and Y. Ribakov, "Influence of various reinforcing arrangements and of gravitation stresses on hysteretic behavior of RC sections," *European Earthquake Engineering*, vol. 3, pp. 13–24, 2005.
- [19] I. Iskhakov and Y. Ribakov, "Experimental and numerical investigation of a full-scale multistorey RC building under dynamic loading," *The Structural Design of Tall and Special Buildings*, vol. 14, no. 4, pp. 299–313, 2005.



Journal of  
Nanotechnology



International Journal of  
Corrosion



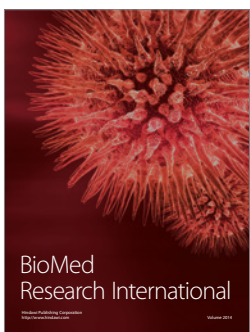
International Journal of  
Polymer Science



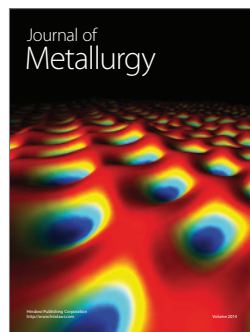
Smart Materials  
Research



Journal of  
Composites



BioMed  
Research International



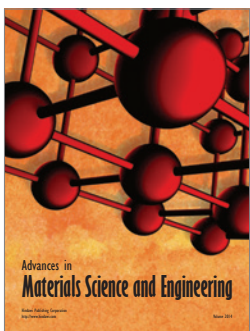
Journal of  
Metallurgy



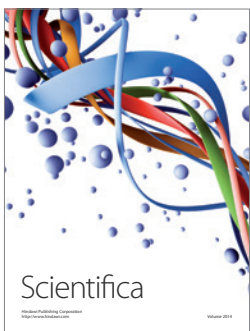
Journal of  
Materials



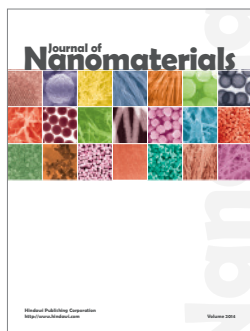
Journal of  
Nanoparticles



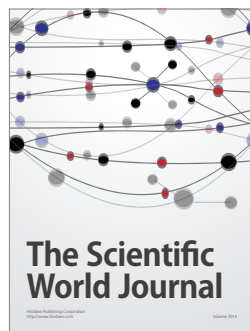
Advances in  
Materials Science and Engineering



Scientifica



Journal of  
Nanomaterials



The Scientific  
World Journal



International Journal of  
Biomaterials



Journal of  
Nanoscience



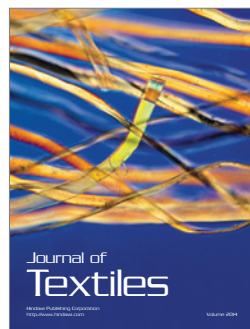
Journal of  
Coatings



Journal of  
Crystallography



Journal of  
Ceramics



Journal of  
Textiles